Stressed Detector Arrays for Airborne Astronomy

G.J. Stacey, J.W. Beeman, E.E. Haller
UC Berkeley
and N. Geis, A. Poglitsch, and M. Rumitz
Max-Planck Institut für Physik und Astrophysik

ABSTRACT. We report on the development of stressed Ge:Ga detector arrays for far-infrared astronomy from the Kuiper Airborne Observatory (KAO). We successfully constructed and used a three channel detector array on five flights from the KAO, and have conducted laboratory tests of a two dimensional, 25 element (5×5) detector array. Each element of the three element array performs as well as our best single channel detector, as do the tested elements of the 25 channel system. Some of the exciting new science possible with far-infrared detector arrays is also discussed.

I. Introduction.

Impurity doped germanium photoconductors have been the primary detective devices for far-infrared (FIR) astronomy for many years. The first FIR line detected from an astronomical source was the 88 μm line of doubly ionized oxygen detected from the M17 HII region in 1975 (Ward et al. 1975). The instrument used was a grating spectrometer with a single Ge:Ga photoconductor as the detector. Haller, Heuschen and Richards (1979) demonstrated that the application of 60 kgf mm^{-2} of stress along the [100] crystalographic axis of these Ge:Ga photoconductors lowers the binding levels of the Gallium impurity sites to about 6 meV, shifting the cutoff wavelength of the detectors from ~120 μm to longward of 200 μm.

Stressed Ge:Ga photoconductors were first used for astronomical spectroscopy by Martin Harwit's group at Cornell in 1979. They reported the first astronomical detection of the important fine structure line of singly ionized carbon at 158 μm the following year (Russell et al. 1980). Stressed detectors have now been used successfully by several groups for astronomical research including efforts at Cornell and NASA Ames in the US, in Japan (c.f. Okuda et al. 1989), at MPA in West Germany and our continuing efforts at UC Berkeley and MPE. The detectors and J-FET transimpedance amplifiers have sufficiently low intrinsic noise figures to insure background limited performance from spectrometers on the airborne and balloon borne observatories for even the highest spectral resolutions employed to date (~20 km s^{-1}). Further improvements in the data rate for these spectrometers then requires the implementation of detector arrays.

More than a dozen FIR molecular rotational lines and atomic fine structure lines have been detected by several research groups with stressed detectors. Several other important lines remain undetected. Of special interest are the several rotational lines of H_2O which lie in the wavelength range between 130 and 220 μm. These lines are inaccessible even at aircraft altitudes due to obscuration by terrestrial water vapor lines. Their detection awaits the introduction of space based FIR spectrometers such as SIRTF and ISO.

We report the design and use of a three element linear array for the UCB tandem Fabry Perot on the KAO, and the design and preliminary laboratory testing of a two dimensional stressed detector array to be used on the KAO in a new very high spectral resolution Fabry Perot system in the summer of 1989.

II. A Very Compact Three Channel Stressed Detector.

In order to improve the data taking efficiency of our tandem Fabry Perot system, we replaced our single channel system with a three element detector array.

A. Design Considerations.

The diffraction limited beam size at 158 μm for the 91.4 cm telescope on the KAO is approximately 45". The plate scale at the detector in the UCB Tandem Fabry Perot is 45" per mm. Therefore, the optimal entrance aperture for our detectors (assuming a point source) is 1 mm. It is easy to demonstrate (c.f. Lugten 1987) that the maximum attainable resolution of a Fabry Perot is limited by the angular divergence of the beam in that Fabry Perot. This divergence rapidly worsens as one goes off axis in the system. To minimize this effect, the off-axis channel must be kept as close as possible to the central ray. It is clearly advantageous to keep the beams as close as possible to one another for sampling purposes as well.

This constraint presents a problem. The detectors themselves are typically 1 mm cubes. The probability for single pass absorption for these size detectors is roughly 5 - 10%. Integrating cavities are therefore required for good quantum efficiency. Furthermore, each detector must be stressed nearly to the breaking point along the [100] axis. To achieve high quantum efficiency for a given wavelength (we choose to optimize for 158 μm operation), this stress must be applied uniformly. This insures the response curve in all parts of the detector peaks at the same wavelength.

We achieved this by stacking individual detectors of the array along the stress axis to form a linear array, enabling stress to be applied along a single axis with a single set screw. Figure 1 illustrates our design. The detector is composed of several simple pieces. Each Ge:Ga crystal, (e), (1 mm cube) is mounted in its own integrating cavity whose walls are a 4.5 mm hole drilled through a 1 mm thick wafer of aluminum. The bottom of the cavity is formed by a 50 μm thick piece of stainless shimstock, (a). The aluminum wafers are then stacked such that the bottom of one detector cavity forms the top of the cavity below. The top cavity is capped by the stainless steel top of the detector housing. The aluminum wafers are copper plated, then soldered to the copper plated stainless steel shim stock. The 32 μm copper plating serves as a cushioning pad for the Ge:Ga detectors along the stress axis. This prevents Ge:Ga breakage due to unavoidable small imperfections in the Ge:Ga crystal and stainless surfaces. Each detector is placed within about 50 μm of the center of its cavity and fixed with indium solder. The corners of the detectors are centered with respect to the entrance pinholes to ensure the first pass of reflected radiation is trapped by the integrating cavity and not reflected directly out through the entrance aperture. The detector housing itself is maintained at constant voltage bias, while the signal end of the detector is electrically isolated from the housing by a 75 μm thick sheet of mica, (c). The electrical connection is obtained with a 25 μm thick sheet of brass, (d), which also serves as a stress pad for the detector. Brass pads have an advantage over copper pads in that they cushion adequately but will not extrude under stress nearly as much as copper pads (Beeman et al. 1989). The brass pad has a 75 μm diameter high thermal impedance (Constantan) wire indium soldered at one corner to complete the electrical circuit. A 100 μm thick, 2 mm diameter disk of stainless steel, (b), is fixed to the bottom of each detector wafer, which prevents "drumhead" distortions of the 50 μm stainless plate as the stress is applied. These distortions would result in non-uniform stress, manifested as a slow responsivity onset at long wavelengths, and non-optimal response over a broad band. Stress is applied through the entire stack of three

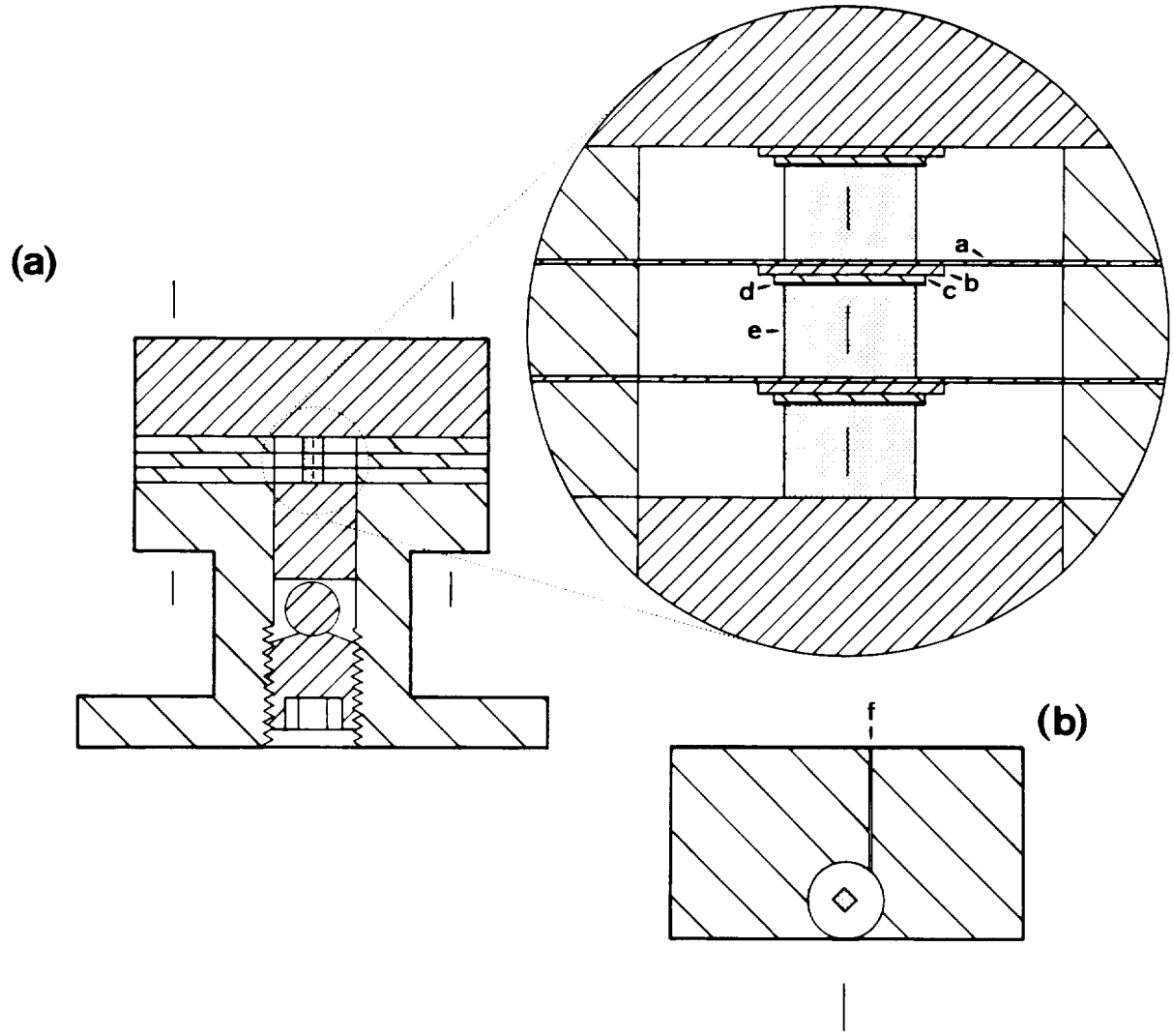

Figure 1. (a) Cutaway drawing of three channel stressed detector array. The inset is an enlarged view of the detector cavities themselves. (b) Top view of a single detector "wafer" shown with the detector installed. (f) is a 250 μm wide, 250 μm deep groove which retains the signal wire.

detectors with a single 1/4" -28 thread set screw. Screw torque is decoupled in the standard manner, a 1/8" stainless steel ball bearing, and stress is delivered through a 4.5 mm diameter piston 5 mm long. The body of the detector is constructed of aluminum alloy which both ensures good thermal conductivity, and results in a large amount of differential thermal contraction between the housing and the stainless steel set screw, ball bearing, plunger and germanium crystal stack. Thus, cooling the detector increases the stress along the detector array axis. The completed detector is shown in Figure 2.

The initial stress on the detector is set at room temperature by measuring the DC impedance of the detector as the screw is tightened. We have found that lowering the impedance to about 85% of its unstressed value results in a responsivity curve which peaks at about 158 μm for this type of detector housing. The differential contraction in the detector housing during cooling will then result in a stress of about 50 kgf mm^2 at 2 K.

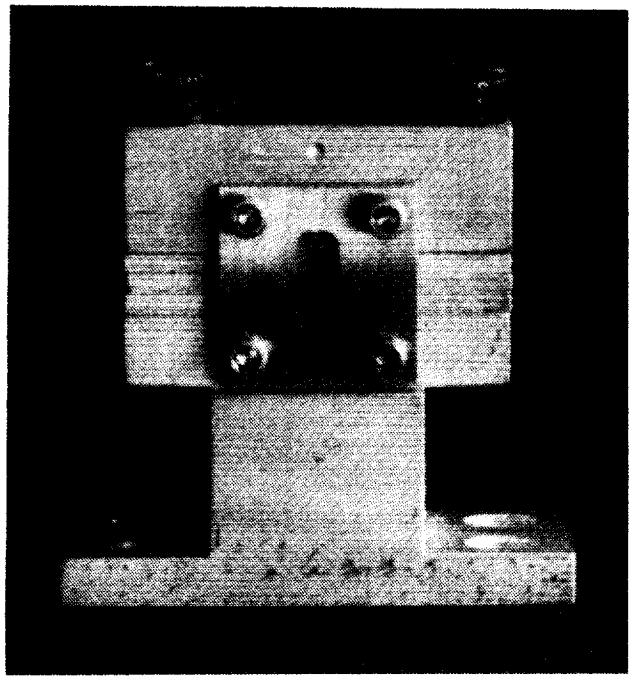

Figure 2. Photograph of the three element linear array. 1 mm pinholes are installed.

TABLE 1

Detector	Cutoff λ	Optimal Bias	Response[1,3]	Noise Equivalent Power[2] Unvignetted[3]	Inflight[4]	
	(microns)	(mV)	(Amp/Watt)	(100 km s^{-1})	(100 km s^{-1})	(40 km s^{-1})
Single Channel	210	15	4.6	3.9	3.9	2.5
Three Channel						
1	215	10	4.1	4.0	5.6	-
2 (central)	220	10	4.9	3.6	3.6	2.3
3	205	10	4.0	3.9	4.6	-
5 x 1 Linear Arrays	212	8	8.5	3.9	-	-

[1] At optimal bias.
[2] In units of 10^{-15} W-$Hz^{-1/2}$, at 158 μm, at the quoted spectral resolutions (FWHM).
[3] For a direct pass through the system; i.e. taking into account known vignetting in the system for the side channels of the three channel detector, but not correcting for walk-off in the Fabry Perot.
[4] Referred to the sky, i.e. including all loses.

B. Three-Element Array Performance

The operating characteristics of the three channel system are similar to the single channel system previously used in the spectrometer (Table 1). At 158 μm, the detector response is ~4 amps/Watt for each channel at the optimal bias voltage (10 mV across the 1mm interelectrode distance). As the detector sensitivity as a function of bias is nearly flat near the optimal bias point, all detectors may be operated at their optimal sensitivity with a common detector bias. The transmission of the entire optical path in the Fabry Perot spectrometer is of the order 16% (Lugten, 1987). With this transmission, and given the background limited performance of the spectrometer, we calculate a quantum efficiency of the order 20% for all of the detectors. Electrical crosstalk has been determined through laboratory measurements at about 1%. Through in flight measurements of Jupiter (42.5" diameter) we have determined the optical crosstalk between detectors, i.e. that percentage of the signal from a point source in one channel which shows up as a edge of the beam signal in the next adjacent channel. The beam overlap is 11% for immediately adjacent channels, and 6% for channels two beams away. The former value is precisely that predicted for a 55" Gaussian beam convolved with the a disk the size of Jupiter (Harris, 1988), while the later number is somewhat larger, consistent with the known extended (non-Gaussian) wings of our FIR beam.

The cutoff wavelengths for each of the three detectors is nearly identical to that of a single stressed detector (~210 μm), the onset is consistent with good uniform stress across the three channels. We measure a system NEP at 158 μm for the central channel of our array which is fully as good as our best single channel NEP (~2-3x10^{-15}W $Hz^{-1/2}$ at 40 km s^{-1} resolution). The side channels have a somewhat higher NEP due to walkoff of the FIR radiation through the FP (c.f. Poglitsch et al. 1989). This problem is not severe at 100 km s^{-1} resolution (factor of 1.3) but rapidly worsens as the divergence limit of the side channel resolution (32 km s^{-1}) is approached.

The detectors are kept at ~2.2 K by pumping on the liquid helium bath. At these temperatures, the dark current is ~3x$10^{6}e^{-1}s^{-1}$. Due to the high background environment on the KAO telescope (equivalent to a 240 K greybody of emissivity 25%) this dark current is an insignificant effect (~10% of the KAO background). We use a standard matched dual J-FET (2N6484) transimpedance amplifier and 2 x 10^{9} Ω ELTEC model 104 load resistors. The silicon J-FETs are mechanically coupled to the helium work surface with thin wall fiberglass tube, and heated to an 80 K operating temperature with a 1kΩ carbon resistor. The detector is shielded from radiation emitted by the heated J-FET assembly with a He temperature copper house around the J-FET "tower". The transimpedance amplifier is essentially microphonic free.

III. A 5x5 Stressed Detector Array.

A. The Triple Fabry Perot Imaging Spectrometer.

As part of a new triple Fabry Perot imaging spectrometer, we have developed a 5x5 stressed detector array. The new Fabry-Perot is a collaborative effort between our laboratories in Berkeley and Munich. The new spectrometer employs several improvements over the tandem Fabry Perot system.

1. We now have a much larger diameter (4 cm vs. 1.6 cm) collimated beam through the scanning Fabry Perot. As the angular divergence of rays in the Fabry Perot goes roughly as the square of the physical size of the collimated beam (assuming diffraction limited beams with the same f-ratio for both systems), the divergence

limit of our new system is approximately eight times better for a given beam size than for the old system. At 158 μm, the divergence limit for the central 40" pixel is of the order 1.5 km s^{-1}. We thus expect to achieve resolutions as high as 2 to 3 km s^{-1} at the [CII] line frequency. At shorter wavelengths, the diffraction limited beam is correspondingly smaller, permitting, for example spectral resolutions as high as 0.5 km s^{-1} at the bright 63.2 μm [OI] line. As with the three channel system, at the highest resolutions the side channels will suffer much more due to off axis rays than the central pixel. The "first ring" of eight pixels has a divergence limit of about 8 km s^{-1}, and the "second ring" of 16 pixels will have a divergence limit of roughly 32 km s^{-1}.

2. We now employ three Fabry Perot interferometers in series to ensure the minimum background radiation on the detectors even at the highest spectral resolution, permitting significant (factor of three to six) improvements in system sensitivity.

3. The focal plane plate scale has been expanded to 4 mm per 40" beam. This expanded scale permits the introduction for the first time of two dimensional detector arrays. These two dimensional spatial arrays offer the advantage over spectral arrays or spatial/spectral arrays of absolute plate scale registry between adjacent pixels in a map.

4. The new spectrometer also features several other new features including: a) Inflight selection of focal plane plate scale, adjustable from 40" to 20" in a few seconds during flight; b) Precise in flight flat fielding with high and low temperature blackbody calibration cells; c) Frequency switched operation of the high order Fabry Perot which permitting accurate mapping of astronomical sources of angular extent larger than the KAO chopper throw.

B. The 5×5 Detector Array Design.

The new 5×5 detector array is essentially an extension of the three detector system. The array is constructed in a stacked manner as with the three channel system, so that the finished detector array consists of five separate 5×1 channel linear arrays. A cutaway of the 5×1 design is illustrated in Figure 3.

The housing is constructed of aluminum alloy. Each detector element, (c), is 1mm × 1mm in cross section and has a 1.5 mm interelectrode distance. Stress is applied by a single torque decoupled set screw through a stainless plunger. The elements in the stack are separated by 3 mm tall close fitting stainless steel plungers which also deliver the stress through the stack. Electrical connection and stress application are achieved in precisely the same manner as with the three element detector array. For all of the detectors in a stack, it is essential that each element have roughly the same cross section through the stress axis, ensuring the uniformity of stress in a stack. It is also important that the plunger walls be both smooth and perpendicular to the stress axis. The detectors themselves must also be cut perpendicular to the stress axis to ensure even application of the stress across the detector face and minimize the probability of breakage.

The focal plane plate scale in the new Fabry Perot is 10" per millimeter. At 158 μm, a diffraction limited beam is therefore ~4 mm in diameter. We use light cones to condense this beam size to a reasonable size entrance pinhole (1 mm) for the detector integrating cavity. The back side of the cone array mates with the detector array and forms a light tight integrating cavity. As with the three element array, all optical elements of the array are plated with a layer of gold 5 μm thick to ensure a corrosion resistant surface of very high reflectivity in the FIR.

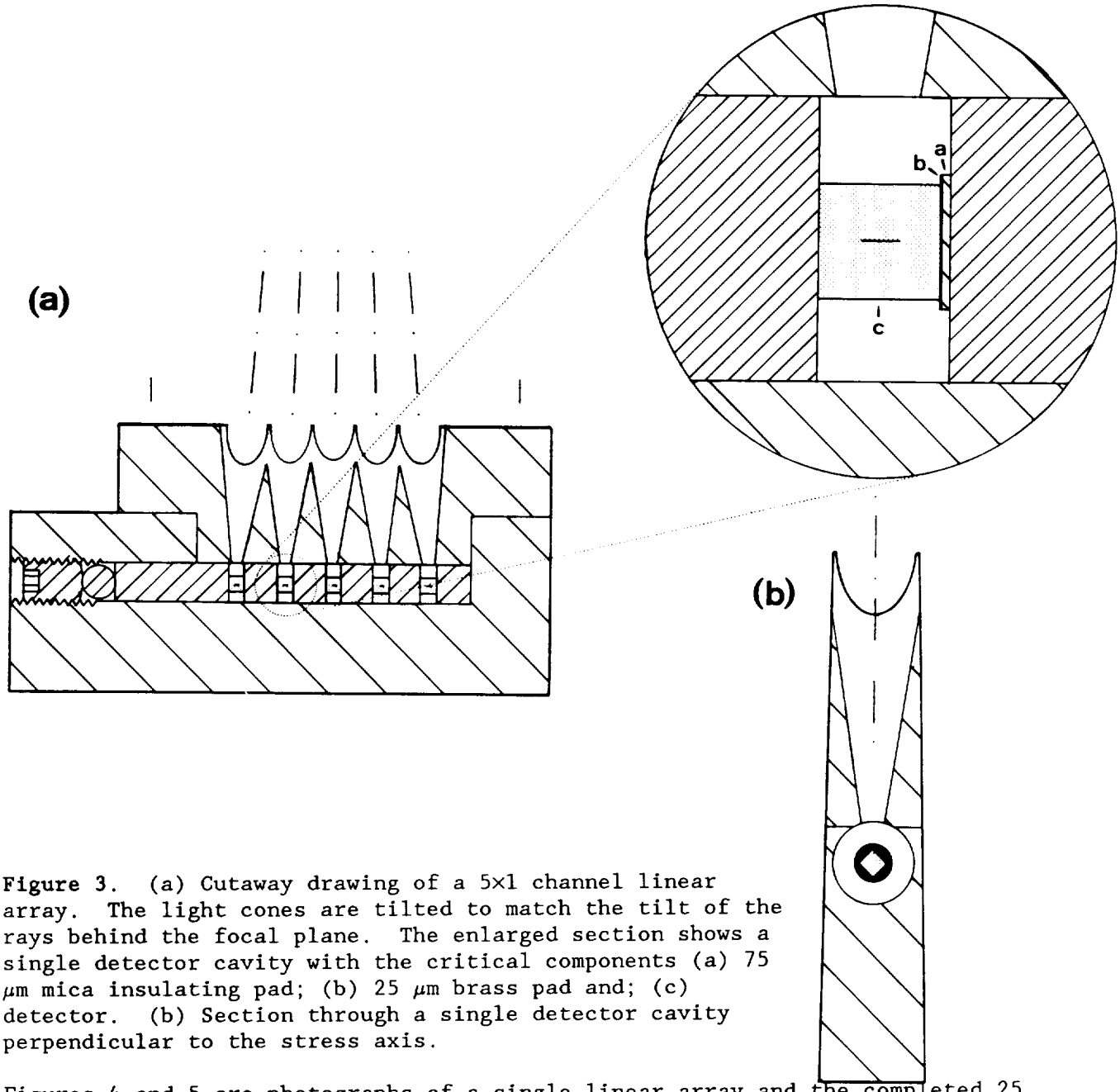

Figure 3. (a) Cutaway drawing of a 5×1 channel linear array. The light cones are tilted to match the tilt of the rays behind the focal plane. The enlarged section shows a single detector cavity with the critical components (a) 75 μm mica insulating pad; (b) 25 μm brass pad and; (c) detector. (b) Section through a single detector cavity perpendicular to the stress axis.

Figures 4 and 5 are photographs of a single linear array and the completed 25 element array respectively. Each array element is identical, and has been designed to be stacked side to side with the adjacent elements. The entire unit makes a reasonably compact unit 8 cm tall and 5 cm wide at the base.

Each linear array is has proven to be easy to assemble. The entire process from cutting the brass pads to stressing the stack takes about two hours per array element. Five stacks have been constructed, each element of which has been thermally cycled to helium temperature at least six times to date with no mechanical failures. The stress on a stack stays constant after about three thermal cycles. Two detectors have been thoroughly tested with respect to sensitivity. Both detectors, the central channel of an array, have 100% of the response and sensitivity of our best single channel detector at both 158 μm and 186 μm, consistent with good uniform stress and high quantum efficiency (Table 1).

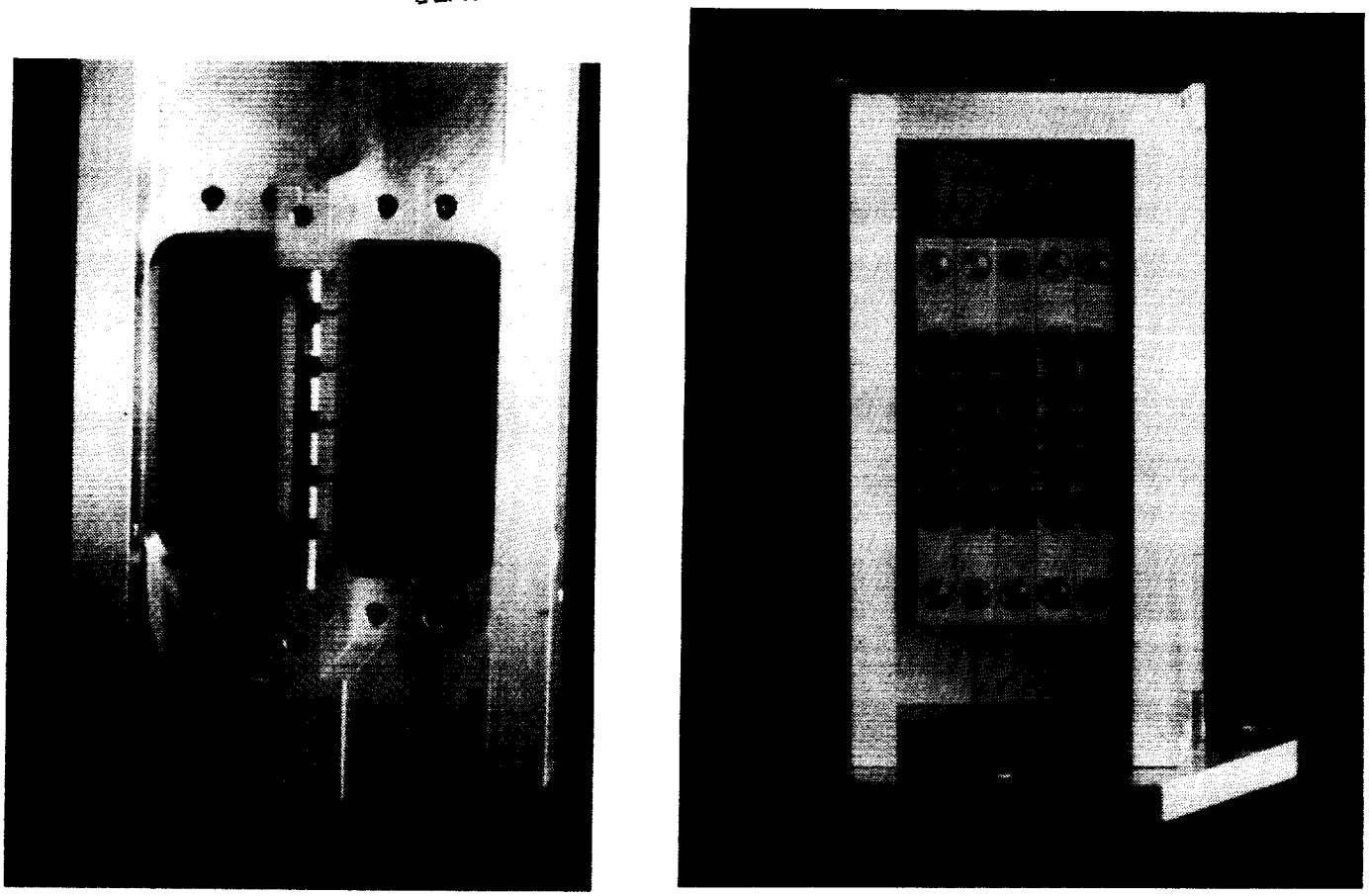

Figure 4. (left) Photograph of a single 5x1 element linear array with the light cone removed.

Figure 5. (right) Completed 5x1 element stressed array with light cones.

IV. Transimpedance Amplifier Arrays

Low noise transimpedance amplifiers (TIA's) which operate at liquid helium temperatures are an important development for detector array technology. Together with the twenty five channel array, a new set of liquid helium temperature transimpedance amplifier arrays has been developed. Each five by one element detector stack has a five channel MESFET transimpedance amplifier securely mounted to its back. These arrays of transimpedance amplifiers consist of five Mitsubishi model 1402 GaAs FET's and five $3 \times 10^9 \Omega$ ELTEC model 112 feedback resistors bonded to a ceramic substrate. These integrated circuits are encased in an aluminum housing which is mechanically attached to the back of each detector array element. The entire assembly makes for a very compact and rugged design. With high input impedance ($>10^{11}\Omega$) and small input noise figures (typically less than 150 nV $Hz^{-1/2}$ at 20 Hz), these transimpedance amplifiers promise to give us background limited performance at even the highest spectral resolutions. As the TIA's are directly mounted to the detector housing, the lengths of the high impedance wires in the TIA circuit are dramatically reduced therefore minimizing microphonics. Further information on the GaAs FET transimpedance amplifiers may be found in a forthcoming publication (Rumitz et al. 1989).

The entire detector block/GaAs transimpedance amplifier stage and spectrometer are in the final stages of testing at present in preparation for a July 1989 KAO flight series.

V. Science with Stressed Detector Arrays.

The three element stressed detector array was flown successfully in flight series during January and June 1988. During these five flights, we have detected six new galaxies in the [CII] line (four of which we have partially mapped), constructed large scale maps of nine galactic molecular clouds in their [CII] line radiation, made the first FIR detection of a rotational line of ^{13}CO and detected FIR ^{12}CO rotational line emission in two galactic sources.

Figure 6 is a 1000 point map of the inner 8′ x 10′ regions of the Orion Nebula in the [CII] line. We obtained this map in about one hour of observing time on the KAO during the first flight with the new array (Stacey et al. 1989b). The map is fully sampled for each of the three detectors. We have calibrated each channel separately, and combined the maps to achieve the composite image. The side channels serve to improve the signal to noise ratio in the central portions of the map and extend the map borders about 1′ in all directions. The least significant contour is about three standard deviations from zero.

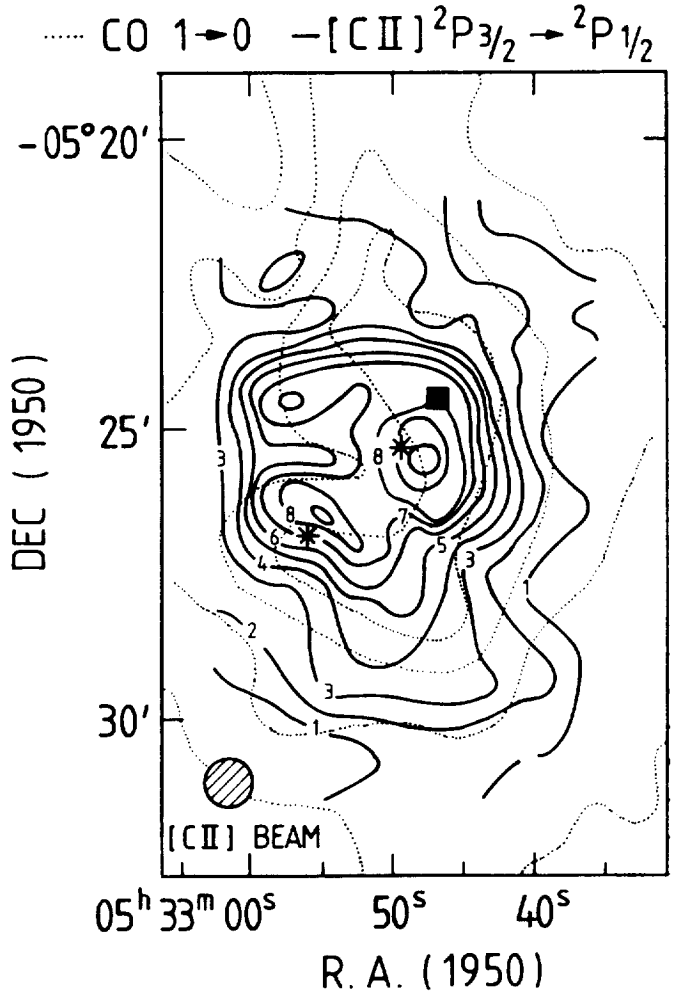

Figure 6. 1000 point [CII] map (dark lines) of the Orion HII/molecular cloud interface region obtained with our 3 detector array in January 1988. The $^{12}CO(J = 1 \rightarrow 0)$ contours (light lines) are from Schloerb et al. 1983).

We have superposed our map on the ^{12}CO (J = 1 - 0) map taken with a similar sized beam by Schloerb et al. 1983. There is excellent agreement between the two maps. The [CII] radiation has been demonstrated to arise in warm (T~500 K) dense (n_{H2} ~ 2 × 10^5 cm^{-3}) photodissociated gas between the visible HII region and the background molecular cloud. The CO line emission traces the molecular gas component. The good spectral and spatial correlation between the two lines indicates that the interface region (traced through its [CII] emission) is physically associated with the "spike" emission seen in the CO line. This supports the contention that this CO emission arises from UV heated warm (T~ 100 K) molecular gas associated with the interface region between the Orion HII region and the bulk of the Orion molecular cloud.

Figure 7 displays a spatially multiplexed spectrum of the starburst galaxy NGC 2146 taken with our three element detector array on its first flight in January 12, 1988 (Stacey et al., 1989b). The array axis was well aligned with the major axis of this highly inclined galaxy: strong [CII] emission is evident from both the nuclear regions (central channel) and regions removed 2.4 kpc away along the galactic major axis (side channels). Strong [CII] line radiation is only consistent with vigorous star formation activity. The large spatial extent of the [CII] radiation in this galaxy indicates that the starburst here is probably not confined to just the galactic nucleus. We have superposed for comparison the $^{12}CO(J = 1 - 0)$ line from this galaxy sampled from the same regions with a similarly sized beam. There is

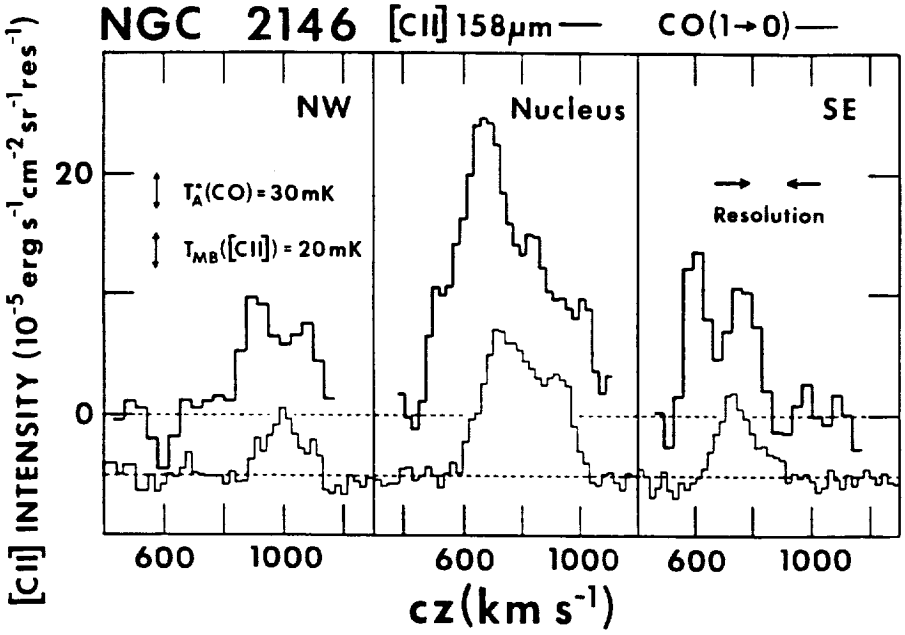

Figure 7. Spatially multiplexed [CII] spectrum (dark lines) of the starburst galaxy NGC 2146 obtained with 22 minutes of integration time with the three channel array. The superposed CO(J = 1 → 0) spectra (light lines) are from Young et al. 1988).

excellent spectral and spatial correlation between the two lines demonstrating that on a galaxy wide scale, the two lines are emitted from similar regions in the galaxy. Notice also that the two lines have a nearly constant line intensity ratio across this galaxy. The line intensity ratio is precisely the same as that obtained for galactic HII regions (e.g. Orion, above).

This result is surprising. The CO line emission from external galaxies is presumed to be dominated by the emission from cold (T~10 K), dark clouds of the galactic "disk". This is the basis for the CO luminosity to mass conversion ratio used for external galaxies. Since there is little UV radiation near these clouds to

photoionize CO and CI to form CII, one would expect very little [CII] line radiation from these cold clouds. This is in fact what we have find for molecular clouds exposed to small UV fields in the Galaxy (Stacey et al. 1989a). On a galaxy wide scale, one would therefore expect a significantly smaller amount of [CII] radiation per unit CO line radiation than for galactic star formation regions. The fact that the line ratio is the same for NGC 2146 (and the nuclei of several other starburst galaxies) as for the Orion HII region indicates that the bulk of the CO line emission from these starburst nuclei may arise in the warm molecular gas associated with star formation regions and not from the cold disk molecular clouds. Thus, for starburst nuclei, the high [CII] to CO line intensity ratio may indicate that the CO line does not purely trace mass but rather traces a combination of mass and molecular gas excitation.

The advantages in a large format detector array for the science described above are evident. The [CII] line radiation from galactic molecular clouds like Orion often extends for substantial fractions of a degree on the sky. Detailed maps of such sources clearly requires a large format array, with its inherent increased data rate (in this case, a factor of 25 over a single channel spectrometer). A 2-dimensional spatial array such as the one described here has the further advantage of absolute registry between pixels in a map. This feature facilitates significantly improved registry between the FIR maps and those obtained with other telescopes in other spectral lines.

Acknowledgements.

We are indebted to the skills of the UC Berkeley machine shop whose talented personnel have made these detectors possible. G.J.S., N.G., A.P., and M.R. thank R. Genzel and C.H. Townes for their enthusiasm and support. We also thank the staff of the Kuiper Airborne Observatory for their usual enthusiasm and especially to W. Whiting for the new programming which allowed us to run with three channels for the first time with minimal pain. We are indebted to A.I. Harris for critical readings of this manuscript. This work was supported by NASA grant NAG2-208.

References

Beeman, J.W., Haller, E.E., Hansen, W.L., Luke, P.N. and Richards, P.L. 1989, this conference.

Lugten, J.B. 1987, Ph.D. thesis, University of California, Berkeley.

Haller, E.E., Hueschen, M.R., and Richards, P.L. 1979, **Appl. Phys. Lett.** 34, 495.

Harris, A.I. 1988, **Intl. J. IR and mm Waves 9**, 231.

Poglitsch, A., Geis, N., Genzel, Haggerty, M.R., Rumitz, M., Stacey, G.J., and Townes, C.H. 1989, in prep.

Okuda, H. et al. 1988, **IAU Symposium NO. 136, The Galactic Center**, M. Morris ed., Springer Verlag.

Rumitz, M. et al. 1989, in prep.

Russell, R.W., Melnick, G., Gull, G.E., and Harwit, M. 1980, **Ap. J. (Letters) 240**, L99.

Schloerb, P.F., Friberg, P., Hjalmarson, A., Hoglund, B., and Irvine, W. M. 1983, **Ap.J. 264**, 161.

Stacey, G.J., Genzel, R., Graf, U., Harris, A.I., Stutzki, J., and Townes, C.H. 1989a, in prep.

Stacey, G.J., Genzel, R., Lugten, J.B., and Townes, C.H. 1989b in prep.

Ward, D.B., Dennison, B., Gull, G., and Harwit, M. 1975, **Ap. J. (Letters) 202**, L31.

Young, J.S., Clausen, M.J., Kleinmann, S.G., Rubin, V.C., and Scoville, N. 1988, **Ap.J. (Letters) 331**, L81.